frontiers in Chemistry

ORIGINAL RESEARCH
published: 05 May 2020
doi: 10.3389/fchem.2020.00334

FeCoNi Sulfides Derived From *In situ* Sulfurization of Precursor Oxides as Oxygen Evolution Reaction Catalyst

Wanqing Teng[1], *Mengtian Huo*[1], *Zhaomei Sun*[1], *Wenrong Yang*[1], *Xiangjiang Zheng*[1]*, *Caifeng Ding*[2]* and *Shusheng Zhang*[1]

[1] *Shandong Provincial Key Laboratory of Detection Technology for Tumor Markers, College of Chemistry and Chemical Engineering, Linyi University, Linyi, China,* [2] *Key Laboratory of Optic-Electric Sensing and Analytical Chemistry for Life Science, Ministry of Education, College of Chemistry and Molecular Engineering, Qingdao University of Science and Technology, Qingdao, China*

It is highly promising to design and develop efficient and economical electrocatalysts for oxygen evolution reaction (OER) in alkaline solution. In this work, we prepare FeCoNi sulfide composites (including FeS, Co_3S_4, and Ni_3S_4) derived from *in situ* sulfurization of precursor oxides on carbon cloth (CC), which are used to become an OER catalyst. Such catalyst shows excellent OER performance, low overpotential, small Tafel slope, and high electrochemical stability, and it is a promising electrocatalyst for OER in alkaline media.

Keywords: oxygen evolution reaction, electrocatalyst, FeCoNi sulfides, nanowires array, *in situ* sulfurization

OPEN ACCESS

Edited by:
Xing Huang,
ETH Zürich, Switzerland

Reviewed by:
Yun Hau Ng,
City University of Hong Kong, Hong Kong
Fatwa Abdi,
Helmholtz-Gemeinschaft Deutscher Forschungszentren (HZ), Germany
Yuxiao Ding,
Max Planck Institute for Chemical Energy Conversion, Germany

***Correspondence:**
Xiangjiang Zheng
zxj4408@126.com
Caifeng Ding
dingcaifeng@qust.edu.cn

Specialty section:
This article was submitted to Catalysis and Photocatalysis, a section of the journal Frontiers in Chemistry

Received: *16 December 2019*
Accepted: *31 March 2020*
Published: *05 May 2020*

Citation:
Teng W, Huo M, Sun Z, Yang W, Zheng X, Ding C and Zhang S (2020) FeCoNi Sulfides Derived From In situ Sulfurization of Precursor Oxides as Oxygen Evolution Reaction Catalyst. Front. Chem. 8:334. doi: 10.3389/fchem.2020.00334

INTRODUCTION

The excessive consumption of fossil energy and the resulting serious environmental problems have triggered strong demand for renewable alternative energy (Chow et al., 2003; Zheng et al., 2014). Hydrogen energy is regarded as a clean and ideal energy carrier that could replace fossil energy (Dresselhaus and Thomas, 2001; Zheng et al., 2017, 2018b). Electrochemical water splitting provides us a promising strategy to largely produce hydrogen (Turner, 2004; Lu et al., 2017). However, hydrogen evolution is seriously restricted by anodic water oxidation due to the multi-electron transfer process and high activation energy barrier (Yin et al., 2010; Yang et al., 2017; Ke et al., 2018; Zheng et al., 2018a; Tang et al., 2019). Therefore, efficient catalysts to reduce activation energy should be developed to boost the water oxidation process. Noble metal oxides (RuO_2 and IrO_2) exhibit excellent catalytic characters in oxygen evolution reaction (OER), but their widespread applications are limited due to scarce resources and high costs (Lee et al., 2012; Reier et al., 2012). Hence, it is necessary to develop efficient and economical OER electrocatalysts.

In recent years, transition-metal oxides and hydroxyl oxide have attracted great interest for catalysts (Lu et al., 2016; Guo et al., 2017; Zhang et al., 2017; Jin et al., 2018; Zhao et al., 2018). Specifically, ferric oxyhydroxide (FeOOH) has shown efficient activity for the OER process (Chemelewski et al., 2014; Luo et al., 2017; Park et al., 2017). Regardless of its abundant reserves and low cost, its performance for OER has certain disparities in comparing with the noble metal catalysts. Many ways have been taken to improve catalysis performance, such as enhancing the conductivity of materials, increasing the specific surface area of materials, doping heteroatom modification, and so on (Feng et al., 2016a,b; Kuang et al., 2017; Li F. et al., 2018). Research shows that transition metal sulfides have better oxygen evolution catalysis performance than oxides because transit metal sulfides have diverse element composition, controllable electronic structure, and fast charge transfer speed (Liu et al., 2016; Chai et al., 2018; Li H. et al., 2018; Zhang et al., 2018).

In this manuscript, we design and develop FeCoNiS sulfides derived from *in situ* sulfurization of precursor oxides on carbon cloth (CC) through two-step hydrothermal methods. At first, FeCoNi-FeOOH nanoarray on CC is prepared through hydrothermal method. Secondly FeCoNiS sulfides derived from *in-situ* sulfurization is prepared through the second hydrothermal method. It shows excellent OER activity needing overpotentials of 220.5 and 269.9 mV to attain current densities of 10 and 100 mA cm^{-2} in 1.0 M KOH. It is a promising electrocatalyst for OER in alkaline media.

RESULTS AND DISCUSSIONS

X-ray diffraction (XRD) patterns of these catalysts are shown in **Figure 1A**. There are two broad diffraction peaks on the bottom curve, which are the amorphous peaks of CC. The middle curve is the XRD pattern of the precursor oxides without sulfide treatment. The peaks at 11.95, 16.87, 26.91, 35.26, 46.69, 56.21, and 64.78° can be indexed to the (110), (200), (310), (211), (411), (521), and (541) planes of FeOOH phase (PDF No. 97-003-1136). The XRD pattern of the product after sulfide treatment is on the top. The diffraction peak intensity is obviously lower than that of the middle curve. For better structural analysis of the product, the powder of the precursor oxides and sulfide products scrapped from CC are characterized by XRD again. XRD curves are shown in **Figures 1B,C**. The main component of precursor oxides is still FeOOH. Considered that Co and Ni are in the precursor, we name the precursor as FeCoNi-FeOOH. The XRD curve of sulfide product shows that there are new phases, including Fe_3O_4 (PDF No.97-005-0272), FeS (PDF No. 04-003-4477), Ni_3S_4 (PDF No. 97-003-6721), and Co_3S_4 (PDF No. 00-047-1738). Part of FeOOH is reduced to Fe_3O_4, so the product is named FeCoNiS-FeO_x.

Scanning electronic microscopy (SEM) pattern of the precursor (FeCoNi-FeOOH) is shown in **Figure 2A**. There are specific and uniform nanowires array on the surface of CC. SEM pattern of FeCoNiS-FeO_x is shown in **Figure 2B**. Obviously, the precursor (FeCoNi-FeOOH) nanowires are smooth, and the product (FeCoNiS-FeO_x) is relatively rough. This means that the product has structural change after sulfidation, which corresponded to the XRD patterns in **Figures 1B,C**. The catalyst nanowire feature is also shown in transmission electron microscopy (TEM) characterization (**Figure 2C**). Image taken from the product shows about 50-nm-thick nanowires. High-resolution TEM (HRTEM) reveals that the product is highly crystallized with well-resolved lattice fringes (**Figure 2D**). The interplanar spacing of 0.331 nm could be assigned to the (310) plane of FeOOH.

The corresponding energy-dispersive X-ray (EDX) elemental mapping images of FeCoNiS-FeO_x are shown in **Figure 3A**, which demonstrate unique distribution of Fe, Co, Ni, and S elements. EDX pattern is shown in **Figure 3B**, which exhibits types and relative amounts of different elements based on the position and intensity of element spectral lines.

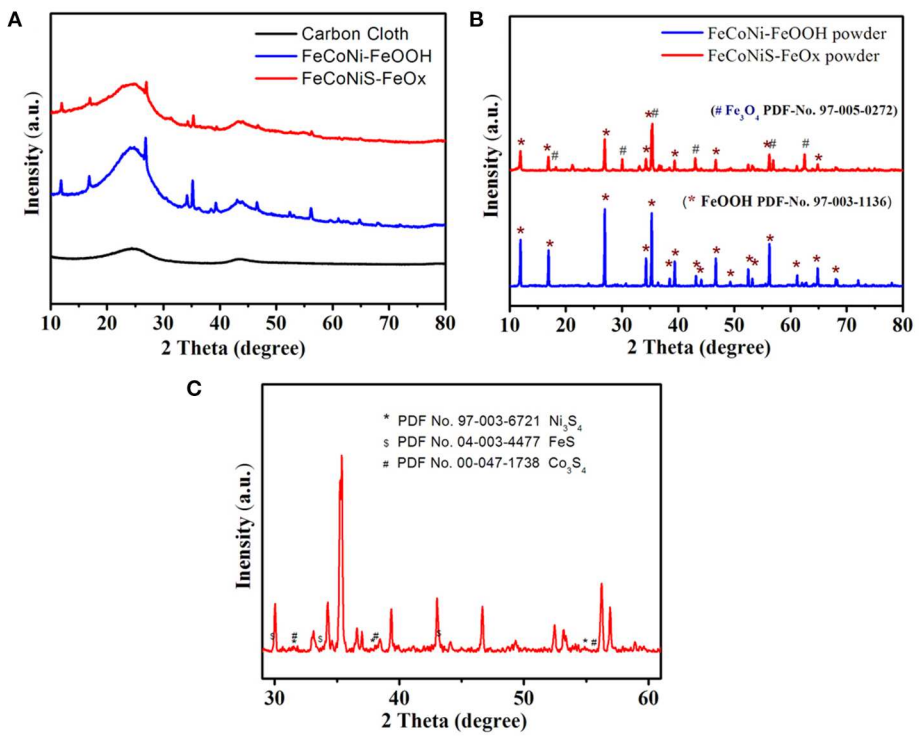

FIGURE 1 | (A) X-ray diffraction (XRD) patterns of different oxygen evolution reaction (OER) catalysts. **(B)** XRD patterns comparison of different catalysts powder. **(C)** XRD pattern of the product after sulfidation treatment.

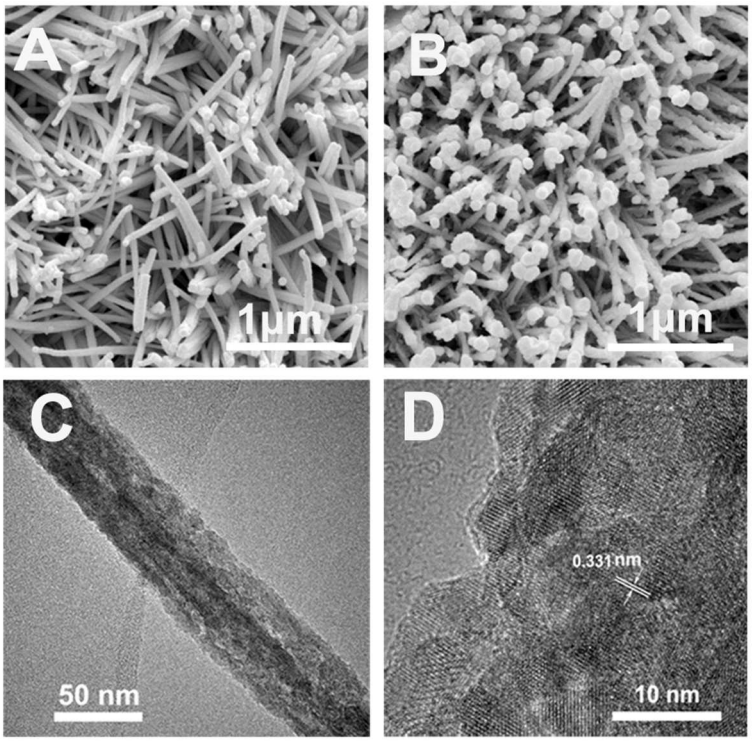

FIGURE 2 | (A) SEM pattern of precursor (FeCoNi-FeOOH). **(B)** SEM pattern of FeCoNiS-FeO_x. **(C)** TEM pattern of FeCoNiS-FeO_x. **(D)** HRTEM pattern of FeCoNiS-FeO_x.

X-ray photoelectron spectroscopy (XPS) of FeCoNiS-FeOOH is shown in **Figure 4**, which was performed to characterize the chemical states of different elements. **Figure 4A** is full-scale XPS spectrum, further revealing the presences of Fe, Co, Ni, S, and O elements in the catalyst. As shown in **Figure 4B**, high-spin Fe^{3+} of FeOOH contains unpaired electrons and therefore exhibit multiplet structures in Fe $2p_{3/2}$ area. The characteristic peaks of Fe $2p_{1/2}$ is at 725.8 eV. The satellite peaks (identified as "Sat.") are at 719.3 and 732.3 eV, which are relevant to Fe $2p_{3/2}$ and Fe $2p_{1/2}$ of FeOOH (Biesinger et al., 2011; Zeng et al., 2012; Zhou et al., 2018). There are two peaks at 714.4 and 723.9 eV, which are relevant to Fe_3O_4. In **Figure 4C**, there exhibit two spin-orbit doublets. The first doublet is at 778.6 and 793.5 eV, assigned to Co $2p_{3/2}$ and Co $2p_{1/2}$ of Co^{3+}, and the second doublet was at 781.9 and 797.8 eV, arising from Co $2p_{3/2}$ and Co $2p_{1/2}$ of Co^{2+}. In addition, two broad peaks located at 803.6 and 786.7 eV are attributed to the satellites, which indicated the presence of Co_3S_4 (Xiao et al., 2014; Liu et al., 2015; Gao et al., 2018; Wang X. et al., 2018).

In the Ni 2p spectrum (**Figure 4D**), there exist two main peaks at 855.7 and 873.5 eV assignable, respectively to Ni $2p_{3/2}$ and Ni $2p_{1/2}$ spin orbit doublets and two satellite peaks (862.4 and 880.1 eV). By deconvolution of the two main peaks, the Ni $2p_{3/2}$ orbit comprises two peaks with binding energy of 853.6 and 856.7 eV, which corresponded, respectively to the Ni^{2+} and Ni^{3+} oxidation states, and the Ni $2p_{1/2}$ orbit can also be fitted into two peaks belonging to Ni^{2+} (871.5 eV) and Ni^{3+} (875.2 eV) (Hu et al., 2015; Qin et al., 2016; Sivanantham et al., 2016). There show S $2p_{3/2}$ and S $2p_{1/2}$ peaks at 161.7 and 162.8 eV in **Figure 4E**, which can be related to S^{2-} (Wang H. et al., 2018). The component peak at 164.1 eV is characteristics of a metal–sulfur (M-S) bond (Ning et al., 2018). The peaks of 168.9 and 170.1 eV can be attributed to SO_4^{2-} due to air oxidation (Cheng et al., 2015). In the O 1s region (**Figure 4F**), the peaks of 530.0, 531.9, and 533.8 eV are observed on the surface of the catalyst, which are corresponding to O^{2-}, hydroxyl group, and adsorbed water molecules, respectively (Luo et al., 2017).

The catalysis performance of the catalyst in water oxidation reaction is evaluated by linear sweep voltammetry (LSV), shown in **Figure 5A**. For comparison, LSV curves of different catalysts with similar loading amounts, including CC, RuO_2, FeCoNi-FeOOH, FeCoNi-FeO_x, FeCoNiS-FeO_x, are also evaluated. Overpotentials in the same current density are often used to estimate the OER performance. FeCoNiS-FeOOH/CC exhibits outstanding OER performance with driving 100 mA cm^{-2} at a low overpotential of 269.9 mV, which is superior to RuO_2/CC and FeCoNi-FeOOH under the same conditions. FeCoNi-FeO_x is prepared through second hydrothermal method without sulfurizing reagent. The OER activity of FeCoNi-FeO_x is lower than FeCoNi-FeOOH. The existence of Fe_3O_4 will not enhance catalytic reactivity. The main active site of FeCoNiS-FeO_x is FeCoNi sulfides. Tafel plots of different OER catalysts were shown in **Figure 5B**, which are used to evaluate the catalytic kinetics. The Tafel slope of FeCoNiS-FeO_x is 45.1 mV dec^{-1}, lower than

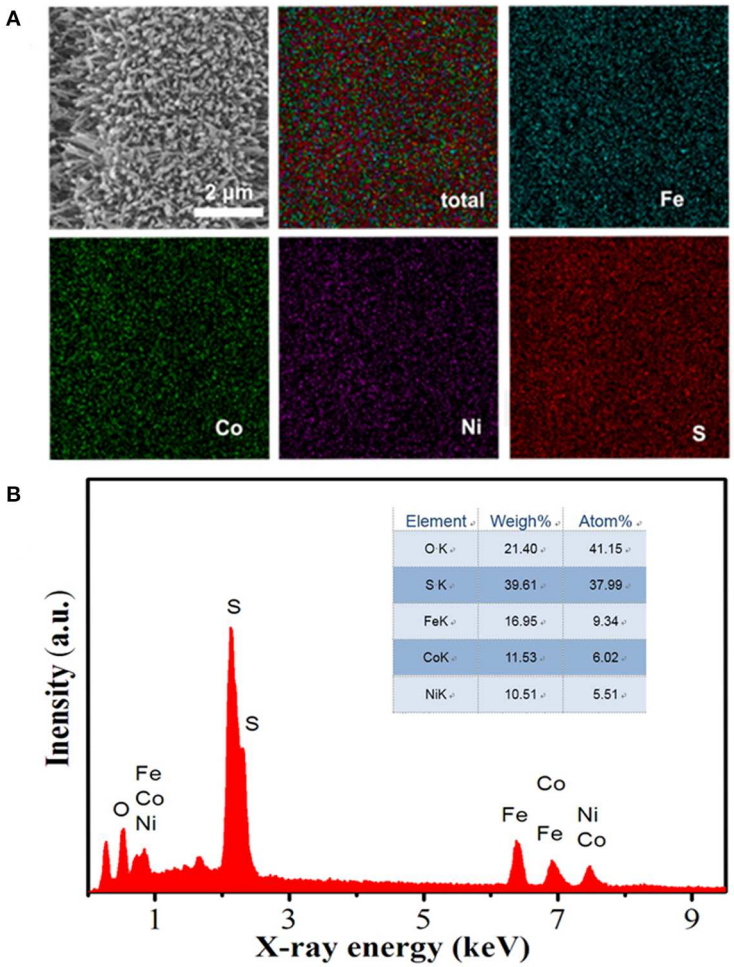

FIGURE 3 | (A) Energy-dispersive X-ray (EDX) mapping images of FeCoNiS-FeOx. **(B)** EDX element distribution pattern.

that of RuO_2/CC (52.3 mV dec^{-1}). It demonstrates that the FeCoNiS-FeO_x catalyst has more rapid reaction velocity in OER catalytic reaction.

Another important performance, stability of catalyst, is investigated by cyclic voltammetry and potentiostatic method. As shown in **Figure 5C**, there shows a comparison of two polarization curves, including original curve and another curve after 500 CV cycles. When the potential is 1.5 V, the current density is only 3% decrease after 500 cycles, which demonstrates that the FeCoNiS-FeO_x catalyst has a good cycle life. In **Figure 5D**, the electrochemical stability of FeCoNiS-FeOOH/CC is tested by potentiostatic electrolysis at a constant potential of 1.48 V for 30 h. There is only 5% decay of current density, which demonstrated the good long-term durability of the catalyst. Multistep chronopotentiometric curve of FeCoNiS-FeO_x is shown in **Figure 6**. There are 12 steps and the increment of current density is 20 mA cm^{-2} per 500 s. In every step, the corresponding potential remains constant. These results indicate that the catalyst has excellent conductivity and good mass transportation.

CONCLUSIONS

In this paper, a two-step hydrothermal routine is adopted to prepare FeCoNiS-FeO_x catalyst. At first, hydroxide nanowire array precursor is prepared. The precursor nanowire arrays serve as backbones for the catalyst not only constructs effective conductive channels but also provides rich active sites. Secondly, the final product is prepared via anion exchange and redox reactions with Na_2S as sulfurizing reagent. The catalyst shows excellent OER activity needing overpotentials of 220.5 and 269.9 mV to attain current densities of 10 and 100 mA cm^{-2} in 1.0 M KOH. Typically, the catalyst also shows long-term electrochemical stability for at least 30 h. The good catalysis performance is due to FeS, Co_3S_4, and Ni_3S_4. CC as substrate could enhance the conductivity of the material. Nanowire structure could increase the surface area of materials and expose more active sites. Most importantly, transition-metal sulfide could optimize material structure and give a full play to the synergy effect between different elements. FeCoNiS-FeO_x catalyst is a promising electrocatalyst for OER in alkaline media.

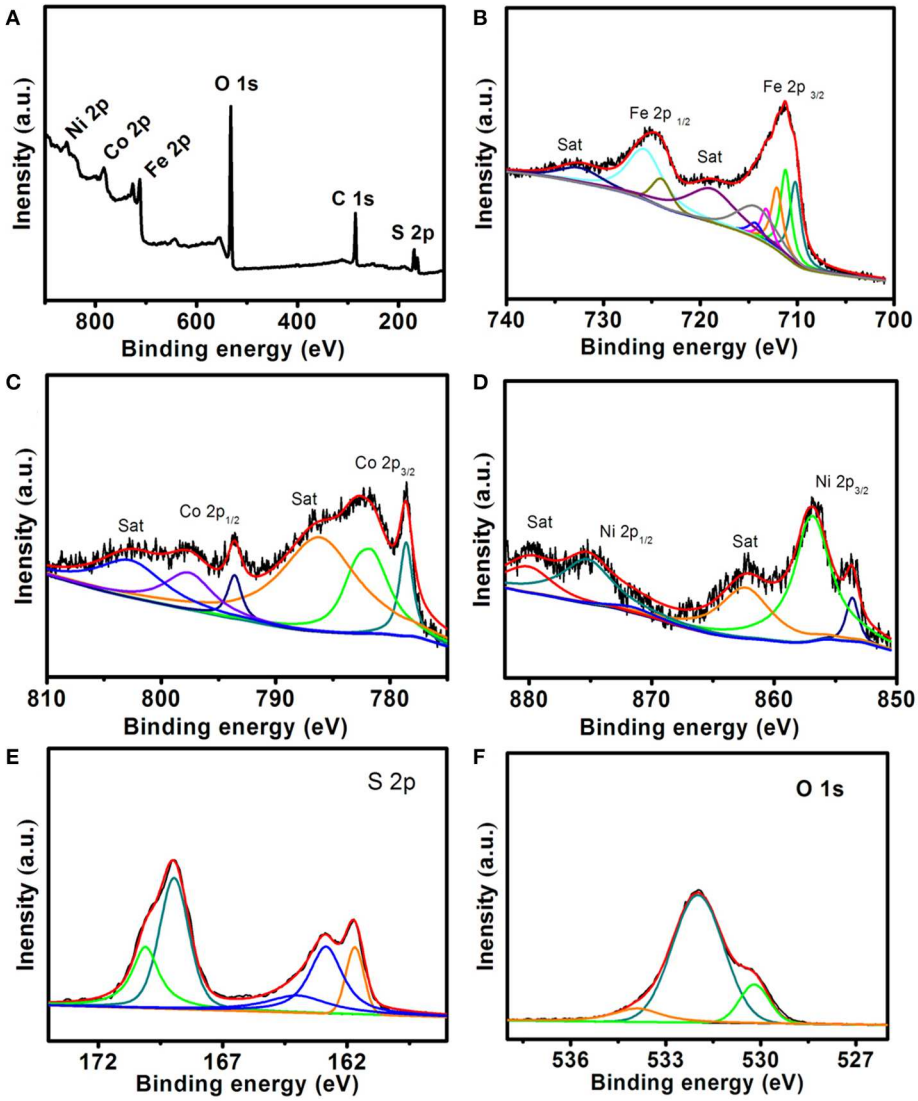

FIGURE 4 | X-ray photoelectron spectroscopy (XPS) spectra of FeCoNiS-FeO_x catalyst. **(A)** Survey spectrum. **(B)** Fe 2p. **(C)** Co 2p. **(D)** Ni 2p. **(E)** S 2p. **(F)** O 1s.

MATERIALS AND METHODS

Materials

Ferric nitrate [$Fe(NO_3)_3.9H_2O$, Mw = 404.00], nickel nitrate [$Ni(NO_3)_2.6H_2O$, Mw = 290.79], cobalt nitrate [$Co(NO_3)_2.6H_2O$, Mw = 291.03], ammonium fluoride NH_4F, Mw = 37.0), urea [$CO(NH_2)_2$, Mw = 60.06], potassium hydroxide (KOH, Mw = 56.1) are provided by Shanghai Aladdin Ltd. Sodium sulfide (Na_2S, Mw = 78.04) and ruthenium chloride ($RuCl_3.3H_2O \geq 43\%$) are bought from Sigma-Aldrich Co. Ltd. CC is supplied by Jingchong electronics technology company. The surface must be free from oil and dirt, then acetone, hydrochloric acid (3 mol/L), ethanol, and ultrapure water are used to clean the surface of CC. Ultrapure water (18.2 MΩ.cm) is used to prepare all aqueous solutions in this work. None of the reagents as received are further purified.

Preparation of Precursor

$Fe(NO_3)_3.9H_2O$ 0.323 g, $Ni(NO_3)_2.6H_2O$ 0.058 g, $Co(NO_3)_2.6H_2O$ 0.058 g, NH_4F 0.03 g, $CO(NH_2)_2$ 0.12 g are added to 20 ml ultrapure water to form mixture solution after 30 min stirring. The final solution and the pretreated CC are sealed in a 30-ml Teflon-lined stainless-steel high-pressure reactor and maintained at 120°C for 5 h. Then, the product is naturally cooled to room temperature. The product is taken from the reactor and washed for three times with ultrapure water and ethanol successively. Dried under 60°C for 2 h.

Preparation of FeCoNiS-FeO_x Nanowire

First, 0.035 g sodium sulfide is added to 20 ml ultrapure water with stirring. The formed solution and the

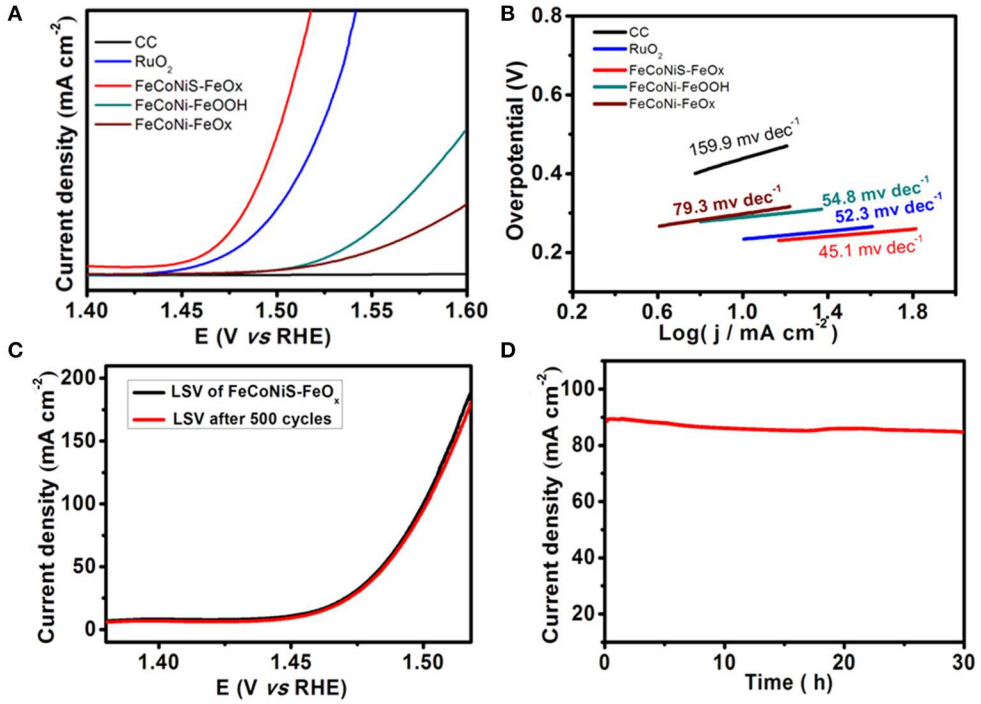

FIGURE 5 | (A) Linear sweep voltammetry (LSV) curves of different oxygen evolution reaction (OER) catalysts. **(B)** Tafel curves of different OER catalysts. **(C)** LSV curve of FeCoNiS-FeO_x catalyst and another curve after 500 CV cycles. **(D)** Time-dependent current density curve of FeCoNiS-FeO_x OER catalyst under constant potential.

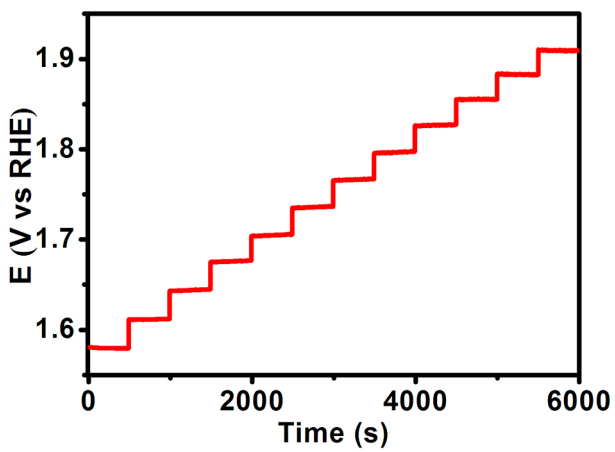

FIGURE 6 | Multistep chronopotentiometric of oxygen evolution reaction (OER) catalyst. The current density started at 60 mA cm^{-2} and finished at 280 mA cm^{-2}, with an increment of 20 mA cm^{-2} per 500 s without ohmic potential drop (IR) correction.

precursor are sealed in a 30-ml Teflon-lined stainless-steel high-pressure reactor and maintain at 120°C for 3 h. After naturally cooling to room temperature, the product is washed with ultrapure water and ethanol successively. At last, the product is dried for 2 h under 60°C.

Characterizations

A diffractometer (RigakuD/MAX 2550, Cu Kα radiation, λ = 1.5418 Å) is used to perform XRD characterization. The scan range is from 5 to 80° with a scanning rate of 5°/min. SEM characterizations are realized on a MERLIN compact SEM with the accelerating voltage of 20 kV. TEM characterizations are realized on TEM of Zeiss Libra 200FE with operation voltage of 200 kV. An ESCALABMK II X-ray photoelectron spectrometer is used to measure XPS spectrum with Mg as the exciting source.

Electrochemical Measurements

A CHI 660E electrochemical analyzer (CH Instruments, Inc., Shanghai) is used to perform all the electrochemical tests. In order to better characterize the electrode reaction, a three-electrode system is adopted. The catalysts/CC is used as working electrode. Mercuric oxide electrode (Hg-HgO) is as contrast electrode. Graphite rod is as auxiliary electrode. Potassium hydroxide solution (1.0 M) is used as the working electrolyte solution. All experiments are realized at 25°C. All potentials for LSV curves are calibrated on reversible hydrogen electrode (RHE) scale [E (RHE) = E + 0.059 × 14 + 0.098]. Unless stated otherwise, all LSV potentials are calibrated with ohmic potential drop (IR) due to solution resistance. Overpotentials (ΔE) are calculated based on the equation ΔE = E (RHE) - IR - 1.23.

DATA AVAILABILITY STATEMENT

All datasets generated for this study are included in the article.

AUTHOR CONTRIBUTIONS

WT has done the experimental work. MH, ZS, and WY helped in characterization. XZ has written the manuscript. CD and SZ have revised the manuscript.

FUNDING

This work was supported by the Natural Science Foundation of Shandong Province (ZR2014BL025).

REFERENCES

Biesinger, M. C., Payne, B. P., Grosvenor, A. P., Lau, L. W. M., Gerson, A. R., and Smart, R. S. C. (2011). Resolving surface chemical states in XPS analysis of first row transition metals, oxides and hydroxides: Cr, Mn, Fe, Co and Ni. *Appl. Surface Sci.* 257, 2717–2730. doi: 10.1016/j.apsusc.2010.10.051

Chai, Y.-M., Shang, X., Liu, Z.-Z., Dong, B., Han, G.-Q., Gao, W.-K., et al. (2018). Ripple-like NiFeCo sulfides on nickel foam derived from *in-situ* sulfurization of precursor oxides as efficient anodes for water oxidation. *Appl. Surface Sci.* 428, 370–376. doi: 10.1016/j.apsusc.2017.09.122

Chemelewski, W. D., Lee, H. C., Lin, J. F., Bard, A. J., and Mullins, C. B. (2014). Amorphous FeOOH oxygen evolution reaction catalyst for photoelectrochemical water splitting. *J. Am. Chem. Soc.* 136, 2843–2850. doi: 10.1021/ja411835a

Cheng, N., Liu, Q., Asiri, A. M., Xing, W., and Sun, X. (2015). A Fe-doped Ni_3S_2particle film as a high-efficiency robust oxygen evolution electrode with very high current density. *J. Mater. Chem. A* 3, 23207–23212. doi: 10.1039/c5ta06788j

Chow, J., Kopp, R. J., and Portney, P. R. (2003). Energy resources and global development. *Science* 302, 1528–1531. doi: 10.1126/science.1091939

Dresselhaus, M. S., and Thomas, I. L. (2001). Alternative energy technologies. *Nature* 414, 332–337. doi: 10.1038/35104599

Feng, J. X., Xu, H., Dong, Y. T., Ye, S. H., Tong, Y. X., and Li, G. R. (2016a). FeOOH/Co/FeOOH hybrid nanotube arrays as high-performance electrocatalysts for the oxygen evolution reaction. *Angew. Chem. Int. Ed Engl.* 55, 3694–3698. doi: 10.1002/anie.201511447

Feng, J. X., Ye, S. H., Xu, H., Tong, Y. X., and Li, G. R. (2016b). Design and synthesis of FeOOH/CeO_2 heterolayered nanotube electrocatalysts for the oxygen evolution reaction. *Adv. Mater.* 28, 4698–4703. doi: 10.1002/adma.201600054

Gao, Z., Chen, C., Chang, J., Chen, L., Wang, P., Wu, D., et al. (2018). Porous Co_3S_4@Ni_3S_4 heterostructure arrays electrode with vertical electrons and ions channels for efficient hybrid supercapacitor. *Chem. Eng. J.* 343, 572–582. doi: 10.1016/j.cej.2018.03.042

Guo, X., Kong, R.-M., Zhang, X., Du, H., and Qu, F. (2017). $Ni(OH)_2$ nanoparticles embedded in conductive microrod array: an efficient and durable electrocatalyst for alkaline oxygen evolution reaction. *ACS Catal.* 8, 651–655. doi: 10.1021/acscatal.7b03406

Hu, Q., Ma, W., Liang, G., Nan, H., Zheng, X., and Zhang, X. (2015). Anion-exchange reaction synthesized $CoNi_2S_4$ nanowires for superior electrochemical performances. *RSC Adv.* 5, 84974–84979. doi: 10.1039/c5ra18625k

Jin, Y., Huang, S., Yue, X., Du, H., and Shen, P. K. (2018). Mo- and Fe-Modified $Ni(OH)_2$/NiOOH nanosheets as highly active and stable electrocatalysts for oxygen evolution reaction. *ACS Catal.* 8, 2359–2363. doi: 10.1021/acscatal.7b04226

Ke, Z., Wang, H., He, D., Song, X., Tang, C., Liu, J., et al. (2018). Co_2P nanoparticles wrapped in amorphous porous carbon as an efficient and stable catalyst for water oxidation. *Front. Chem.* 6:580. doi: 10.3389/fchem.2018.00580

Kuang, M., Wang, Q., Ge, H., Han, P., Gu, Z., Al-Enizi, A. M., et al. (2017). $CuCoO^x$/FeOOH Core–shell nanowires as an efficient bifunctional oxygen evolution and reduction catalyst. *ACS Energy Lett.* 2, 2498–2505. doi: 10.1021/acsenergylett.7b00835

Lee, Y., Suntivich, J., May, K. J., Perry, E. E., and Shao-Horn, Y. (2012). Synthesis and activities of rutile IrO_2 and RuO_2 nanoparticles for oxygen evolution in acid and alkaline solutions. *J. Phys. Chem. Lett.* 3, 399–404. doi: 10.1021/jz2016507

Li, F., Du, J., Li, X., Shen, J., Wang, Y., Zhu, Y., et al. (2018). Integration of FeOOH and Zeolitic imidazolate framework-derived nanoporous carbon as an efficient electrocatalyst for water oxidation. *Adv. Energy Mater.* 8:1702598. doi: 10.1002/aenm.201702598

Li, H., Chen, S., Zhang, Y., Zhang, Q., Jia, X., Zhang, Q., et al. (2018). Systematic design of superaerophobic nanotube-array electrode comprised of transition-metal sulfides for overall water splitting. *Nat. Commun.* 9:2452. doi: 10.1038/s41467-018-04888-0

Liu, D., Lu, Q., Luo, Y., Sun, X., and Asiri, A. M. (2015). NiCo2S4 nanowires array as an efficient bifunctional electrocatalyst for full water splitting with superior activity. *Nanoscale* 7, 15122–15126. doi: 10.1039/c5nr04064g

Liu, T., Sun, X., Asiri, A. M., and He, Y. (2016). One-step electrodeposition of Ni–Co–S nanosheets film as a bifunctional electrocatalyst for efficient water splitting. *Int. J. Hydr. Energy* 41, 7264–7269. doi: 10.1016/j.ijhydene.2016.03.111

Lu, W., Liu, T., Xie, L., Tang, C., Liu, D., Hao, S., et al. (2017). *In situ* derived CoB nanoarray: a high-efficiency and durable 3D bifunctional electrocatalyst for overall alkaline water splitting. *Small* 13:1700805. doi: 10.1002/smll.201700805

Lu, Z., Qian, L., Xu, W., Tian, Y., Jiang, M., Li, Y., et al. (2016). Dehydrated layered double hydroxides: Alcohothermal synthesis and oxygen evolution activity. *Nano Res.* 9, 3152–3161. doi: 10.1007/s12274-016-1197-4

Luo, W., Jiang, C., Li, Y., Shevlin, S. A., Han, X., Qiu, K., et al. (2017). Highly crystallized α-FeOOH for a stable and efficient oxygen evolution reaction. *J. Mater. Chem. A* 5, 2021–2028. doi: 10.1039/c6ta08719a

Ning, Y., Ma, D., Shen, Y., Wang, F., and Zhang, X. (2018). Constructing hierarchical mushroom-like bifunctional NiCo/$NiCo_2S_4$@NiCo/Ni foam electrocatalysts for efficient overall water splitting in alkaline media. *Electrochim. Acta* 265, 19–31. doi: 10.1016/j.electacta.2018.01.150

Park, G., Kim, Y. I., Kim, Y. H., Park, M., Jang, K. Y., Song, H., et al. (2017). Preparation and phase transition of FeOOH nanorods: strain effects on catalytic water oxidation. *Nanoscale* 9, 4751–4758. doi: 10.1039/c6nr09790a

Qin, Z., Chen, Y., Huang, Z., Su, J., Diao, Z., and Guo, L. (2016). Composition-dependent catalytic activities of noble-metal-free NiS/Ni_3S_4 for hydrogen evolution reaction. *J. Phys. Chem. C* 120, 14581–14589. doi: 10.1021/acs.jpcc.6b05230

Reier, T., Oezaslan, M., and Strasser, P. (2012). Electrocatalytic Oxygen Evolution Reaction, (OER). on Ru, Ir, and Pt catalysts: a comparative study of nanoparticles and bulk materials. *ACS Catal.* 2, 1765–1772. doi: 10.1021/cs3003098

Sivanantham, A., Ganesan, P., and Shanmugam, S. (2016). Hierarchical $NiCo_2S_4$nanowire arrays supported on ni foam: an efficient and durable bifunctional electrocatalyst for oxygen and hydrogen evolution reactions. *Adv. Funct. Mater.* 26:201600566. doi: 10.1002/adfm.201600566

Tang, Y., Zheng, S., Xue, H., and Pang, H. (2019). Regulation of the Ni(2+). Content in a Hierarchical Urchin-Like MOF for high-performance electrocatalytic oxygen evolution. *Front. Chem.* 7:411. doi: 10.3389/fchem.2019.00411

Turner, J. A. (2004). Sustainable hydrogen production. *Science* 305, 972–974. doi: 10.1126/science.1103197

Wang, H., Yang, J., Yang, L., Zhang, G., Liu, C., Tang, H., et al. (2018). FeCoNi sulphide-derived nanodots as electrocatalysts for efficient oxygen evolution reaction. *Funct. Mater. Lett.* 11:1850058. doi: 10.1142/s1793604718500583

Wang, X., Liu, C., Li, Q., Li, H., Xu, J., Chu, X., et al. (2018). 3D Heterogeneous Co_3O_4@Co_3S_4 Nanoarrays grown on Ni Foam as a binder-free electrode for lithium-ion batteries. *ChemElectroChem* 5, 309–315. doi: 10.1002/celc.201701050

Xiao, J., Wan, L., Yang, S., Xiao, F., and Wang, S. (2014). Design hierarchical electrodes with highly conductive $NiCo_2S_4$ nanotube arrays grown on carbon fiber paper for high-performance pseudocapacitors. *Nano Lett.* 14, 831–838. doi: 10.1021/nl404199v

Yang, L., Xie, L., Ren, X., Wang, Z., Liu, Z., Du, G., et al. (2017). Hierarchical $CuCo_2S_4$ nanoarrays for high-efficient and durable water oxidation electrocatalysis. *Chem. Commun.* 54, 78–81. doi: 10.1039/c7cc07259g

Yin, Q., Tan, J. M., Besson, C., Geletii, Y. V., Musaev, D. G., Kuznetsov, A. E., et al. (2010). A fast soluble carbon-free molecular water oxidation catalyst based on abundant metals. *Science* 328, 342–345. doi: 10.1126/science.1185372

Zeng, L., Ren, W., Zheng, J., Wu, A., and Cui, P. (2012). Synthesis of water-soluble FeOOH nanospindles and their performance for magnetic resonance imaging. *Appl. Surface Sci.* 258, 2570–2575. doi: 10.1016/j.apsusc.2011.10.093

Zhang, L., Zhang, R., Ge, R., Ren, X., Hao, S., Xie, F., et al. (2017). Facilitating active species generation by amorphous NiFe-Bi layer formation on NiFe-LDH nanoarray for efficient electrocatalytic oxygen evolution at alkaline pH. *Chem. A Eur. J.* 23, 11499–11503. doi: 10.1002/chem.201702745

Zhang, S., Sun, Y., Liao, F., Shen, Y., Shi, H., and Shao, M. (2018). Co_9S_8-CuS-FeS trimetal sulfides for excellent oxygen evolution reaction electrocatalysis. *Electrochim. Acta* 283, 1695–1701. doi: 10.1016/j.electacta.2018.07.133

Zhao, Q., Yang, J., Liu, M., Wang, R., Zhang, G., Wang, H., et al. (2018). Tuning electronic Push/Pull of Ni-based hydroxides to enhance hydrogen and oxygen evolution reactions for water splitting. *ACS Catal.* 8, 5621–5629. doi: 10.1021/acscatal.8b01567

Zheng, X., Song, X., Wang, X., Zhang, Z., Sun, Z., and Guo, Y. (2018a). Nickel–copper bimetal organic framework nanosheets as a highly efficient catalyst for oxygen evolution reaction in alkaline media. *N. J. Chem.* 42, 8346–8350. doi: 10.1039/c8nj01035h

Zheng, X., Zhang, J., Sun, Z., Zhang, Z., and Xi, D. (2018b). Fabrication of Amorphous Cu-Co-P Nanofilms on $CuCo_2O_4$ anoarrays by *in situ* electrochemical reduction for efficient hydrogen evolution in alkaline solution. *Eur. J. Inorg. Chem.* 2018, 3565–3569. doi: 10.1002/ejic.201800492

Zheng, Y., Jiao, Y., Zhu, Y., Cai, Q., Vasileff, A., Li, L. H., et al. (2017). Molecule-level g-C_3N_4 coordinated transition metals as a new class of electrocatalysts for oxygen electrode reactions. *J. Am. Chem. Soc.* 139, 3336–3339. doi: 10.1021/jacs.6b13100

Zheng, Y., Jiao, Y., Zhu, Y., Li, L. H., Han, Y., Chen, Y., et al. (2014). Hydrogen evolution by a metal-free electrocatalyst. *Nat. Commun.* 5:3783. doi: 10.1038/ncomms4783

Zhou, Q., Chen, Y., Zhao, G., Lin, Y., Yu, Z., Xu, X., et al. (2018). Active-site-enriched iron-doped Nickel/Cobalt hydroxide nanosheets for enhanced oxygen evolution reaction. *ACS Catalysis* 8, 5382–5390. doi: 10.1021/acscatal.8b01332

Conflict of Interest: The authors declare that the research was conducted in the absence of any commercial or financial relationships that could be construed as a potential conflict of interest.